ELSEVIER

Inorganica Chimica Acta 225 (1994) 305–317

Inorganica Chimica Acta

Electron transfer reactions in non-stoichiometric ceria and urania

Trevor R. Griffiths*, Hugh V.St.A. Hubbard[1], Mervyn J. Davies[2]

School of Chemistry, University of Leeds, Leeds LS2 9JT, UK

Received 31 March 1994

Abstract

The fluorite oxides ceria and urania can be made non-stoichiometric by loss and gain, respectively, of oxygen atoms, thereby forming CeO_{2-x} and UO_{2+x}. The former now contains Ce^{3+} and Ce^{4+} ions and both single crystal and powder forms are blue and exhibit electron transfer in the form of intervalence spectra. The absorption spectra of pure and reduced ceria crystals are interpreted and used to help resolve electrical conductivity studies. Solid solutions of ceria and urania are blue–black and here electron transfer is of the form $Ce(IV)+U(IV) \rightarrow Ce(III)+U(V)$. The intervalence contribution to the absorption spectrum of ultra-thin single crystal wafers of UO_{2+x} is only available as a difference spectrum, using the UO_2 spectrum as reference. The U^{5+} ions formed and contributing to the intervalence spectra in freshly oxidised samples, quenched from UO_{2+x} at high temperature, were found to be metastable at ambient temperature and slowly oxidised to U^{6+}. The intervalence spectral profile changed significantly and slowly with time. Thus in aged crystals the electron transfer in the intervalence spectrum is principally due to $U(IV)+U(VI) \rightarrow U(V)+U(V)$. Monitoring these changes should yield information on the precipitation of interstitial clusters containing oxygen out of the urania matrix into aggregates and hence the growth as U_3O_7 on surfaces and at grain boundaries.

Keywords: Ceria compounds; Urania compounds; Non-stoichiometric compounds; Intervalence spectra; Interstitial clusters

1. Introduction

Many compounds containing an element in two different oxidation states have long been observed to be intensely coloured. Prussian Blue is probably one of the oldest known. The binary fluorite oxides CeO_2 and UO_2 readily deviate from stoichiometry, forming blue and black materials, respectively. CeO_2 deviates in the direction of oxygen deficiency, CeO_{2-x}, and UO_2 in the direction of oxygen excess, UO_{2+x}. The absorption spectra of reduced ceria has not previously been reported. UO_2 and the U–O system have of course been much studied both theoretically and experimentally for many years but transmission spectra of the black material have been difficult to acquire. We have recently reported a preliminary study identifying an intervalence band in urania [1]. In this study we investigate intervalence bands and processes in hypostoichiometric CeO_{2-x} and hyperstoichiometric UO_{2+x}.

Comprehensive reviews have been written on intervalence bands [2,3]. Robin and Day [2] approached the problem as one concerning the extent of delocalisation of the valence electrons of the mixed valence ions as a means of accounting qualitatively for such physical properties as absorption spectra, electrical conductivity and magnetic properties. Factors which affect the extent of delocalisation are differences in field strength, or symmetry of the ligands surrounding the ions in the two oxidation states, and the distances separating these ions. They classified mixed valence compounds into three types, termed classes I, II and III, based on their physical properties, the strength and symmetry of the ligand fields about the metal ions and the extent of delocalisation of the valence shell electrons. In class I compounds, the ions of differing valence are in sites of very different symmetry and ligand field strength. In class III compounds, the metal ions are in exactly equivalent sites, and with complete delocalisation of donor and acceptor sites. In class II compounds, the metal ions are at distinguishable sites of similar symmetry and ligand field and although there

*Corresponding author.

[1]Present address: IRC in Polymer Science and Engineering, University of Leeds, Leeds LS2 9JT, UK.

[2]Present address: Pilkington Research Laboratories, Lathom, Nr. Ormskirk, Lancs. L40 5UF, UK.

SSDI 0020-1693(94)04062-Z

is some delocalisation of the valence electrons the interaction between the metal ions is weak.

Electron transfer between two different oxidation states in oxides having the fluorite lattice has the characteristics assigned to class II. This is an intermediate classification in which the ions of different oxidation states are distinguishable but are in sites of similar symmetry and ligand field. There is therefore only a small amount of delocalisation of the valence electrons.

1.2. Intervalence spectra

Class II compounds exhibit intense absorption spectra, often in the visible region, that are not characteristic of the element in either or any oxidation state. Such absorption has been termed mixed valence or intervalence absorption (we shall use the latter term). Bands characteristic of the oxidation states of the element are also often observable. Intervalence absorption may be described as the transfer of an optically excited electron from an ion in a lower oxidation state to a neighbouring ion in a higher oxidation state. Such transitions can also occur by thermal activation, and have been used to account for the semi-conductive behaviour found in class II compounds [4].

Allen and Hush [3] have reviewed class II compounds and subdivided them into three types: symmetrical and unsymmetrical homonuclear intervalence transfer, and heteronuclear intervalence transfer. In the first type one electron transfers between ions differing in oxidation state by unity. In the unsymmetrical transfer the difference in oxidation state of the two ions before electron transfer is greater than unity. In heteronuclear intervalence transfer the electron transfers between ions of different elements. In the symmetric homonuclear intervalence transfer the overall energy change is zero provided the two ions are in identical sites. Thus, for an optical transition, the energy must be absorbed almost completely into the phonon system rather than into the electronic levels of the ions.

The theory of intervalence transfer for class II compounds may be discussed using a single frequency model in the high temperature limit (generally ambient or above) with the aid of a configurational coordinate diagram, (Fig. 1). In Fig. 1(a) the overall energy change is E_o, and Fig. 1(b) shows the case for symmetrical electron transfer between cations in identical sites where E_o is zero. It is assumed that the valence electron is coupled with two independent oscillators of identical frequency, ω. The initial and final state equilibrium points are Q_g and Q_e, respectively. The optical absorption transition, of energy E_a, is shown as a vertical line in accordance with the Frank–Condon principle and the radiationless thermal transition, of activation energy, E_t, occurs at the point A. In the high temperature

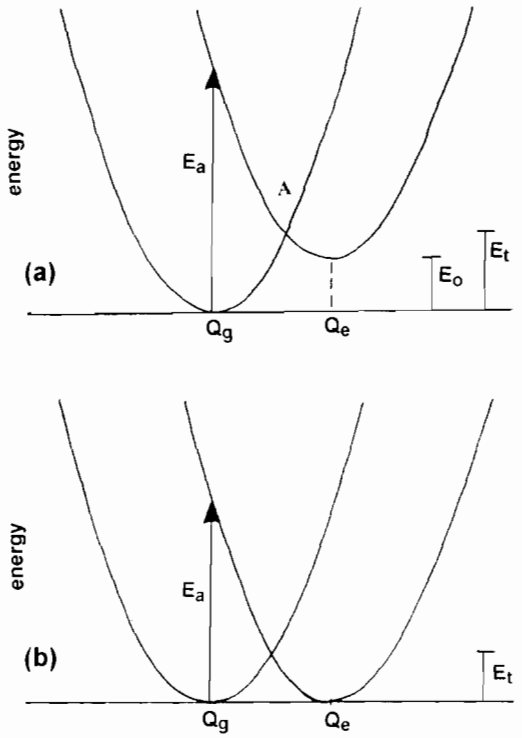

Fig. 1. Configurational coordinate diagram for intervalence transfer processes of overall energy change E_o. (a) $E_o > 0$; (b) $E_o = 0$.

limit at which $kT \gg h\omega$, the optical and thermal energies are related by

$$E_t = [(E_a)^2/4(E_a - E_o)] \quad (1)$$

and the optical absorption band tends to the skewed Gaussian form

$$\alpha = \alpha_o(\nu/\nu_o) \exp[-(E_a - h\nu)^2/4E_p kT] \quad (2)$$

where α is the absorption coefficient, $\nu_o = E_a/h$ and $E_p = E_a - E_o$. Since the bands are usually broad, the band half-width, $\Delta E_{1/2}$, is related to the temperature by

$$\Delta E_{1/2} = (16 \ln 2)^{1/2}(E_p kT)^{1/2} \quad (3)$$

Thus if $E_o = 0$, the maximum absorption frequency may be calculated from the half-width

$$\nu_o(\mathrm{cm}^{-1}) = [\nu_{1/2}(\mathrm{cm}^{-1})]^2/7.7T(\mathrm{K}) \quad (4)$$

Hush [5] has calculated the heats of activation, E_t, for electron transfers between pairs of ions in aqueous solution for various transition metal, M^{3+}/M^{2+}, and actinide, M^{4+}/M^{3+}, ions at 300 K, and deduced values for ν_o lying in the range 12 000–17 000 cm^{-1} with half-widths in the range 5300–6600 cm^{-1}.

1.3. Intervalence transitions in fluorite lattice oxides

Of the three oxides having the fluorite lattice, ceria, thoria and urania, only pure thoria cannot exhibit

intervalence bands since thorium manifests only the (+4) oxidation state. We have therefore elected to report on our findings involving ceria and urania. While electron transfer reactions can arise in thoria subjected to fast particle bombardment [6] we have here chosen to discuss only intervalence spectra related to non-irradiated fluorite oxides.

All three types of electron transfer described by Allen and Hush [3] are possible for ceria and urania. Cerium, showing (+3) and (+4) oxidation states, allows symmetrical homonuclear electron transfer in reduced ceria, CeO_{2-x}, with oxide lattice vacancies available for electrical neutrality.

Symmetrical homonuclear electron transfer can also appear in oxidised urania, UO_{2+x}, since uranium shows the (+4), (+5) and (+6) oxidation states. In addition, unsymmetrical electron transfer is possible between U(IV) and U(VI). The third type, heteronuclear intervalence transfer, is possible in CeO_2–UO_2 solid solutions.

When a crystal of UO_{2+x} contains interstitial oxygen ions, U^{5+} and/or U^{6+} ions are formed to maintain electrical neutrality. The entry of these interstitial ions results in defect cluster formation. Initially 2:1:2 clusters appear as excess oxygen enters the lattice, and these only become 2:2:2 clusters when x in UO_{2+x} reaches ~ 0.1 [1]. The cation lattice remains fixed in position, but some uranium ions are now surrounded differently by interstitial oxygen compared with the majority of uranium ions in the lattice. Thus this makes for a complicated electron transfer absorption spectrum, which is further complicated by the superimposition of the 5f–5f transitions of the U^{4+} and U^{5+} ions. Reduced ceria, CeO_{2-x}, also has a rigid cation lattice, and oxygen atoms missing from sites in the anion lattice. One (or less likely both) of the remaining electrons previously associated with the each of the missing atoms will reduce one of the nearest neighbour cations to Ce^{3+}. The subsequent electron transfer spectrum is therefore much simpler.

2. Experimental

2.1. Crystals and crystal preparation

The single crystals of cerium dioxide were obtained from Dr G.W. Clark, Oak Ridge National Laboratory, TN, USA. They were grown from a tungstate flux and contained tungsten 100–200 ppm, lithium 50 ppm and silicon <50 ppm. The crystals were light blue in colour and varied in size from 0.5 to 2.0 mm^3. Some similarly sized but essentially pure crystals were obtained that had been plasma-fused from pure ceria: these were colourless. Flux-grown crystals doped with the rare-earth oxides Nd_2O_3 and Dy_2O_3 were also colourless.

Small irregular single crystals of UO_2 of around 0.3 cm^3 were prepared by arc-fusion and provided by Dr B.T.M. Willis, Atomic Energy Establishment, Harwell, U.K. Spectrographic analysis revealed impurity concentrations for sodium, silicon and platinum below 0.1%, between 200 and 800 ppm for the various lanthanides present and well below 100 ppm for other elements identified. Later, single crystals were obtained from the Norton Research Corporation, Chippawa, Canada, and were reportedly found in the centre of a two ton mass of depleted UO_2 which had been allowed to cool slowly after being made molten by arc-fusion using carbon electrodes. As supplied, the crystals were irregular pieces of around 1 to 3 cm^3. Samples were analysed at Harwell and carbon was found at 240 ppm, with hafnium, thorium, cerium and zirconium below 100 ppm.

The black urania crystals had to be sectioned and ground down to very thin wafers for transmission studies. The original crystals were cut by Harwell on a diamond slitting wheel into 5–10 thin sections, each of thickness 100–500 μm. Many sections broke at this stage but the largest were then attached to a silica slide mounted on a piston with either Lakeside 70 or Crystal-bond 509. The exposed face was then hand-ground flat on a glass plate using 1200 mesh silicon carbide as abrasive and water as lubricant. The piston was fitted into a sleeve to keep the face perfectly flat against the glass plate and to maintain a constant pressure on the crystal face. This face was then polished on a Selvet cloth, progressively, using 5, 2, 0.3 and 0.05 μm Lindé alumina as polishant.

The resin was then dissolved, the crystal removed, reversed, reattached to the slide and ground to the required thickness. The thickness was monitored by using both a Geiger counter and visually. When viewed in transmitted light the crystals varied from deep red through yellow–orange to transparent as the crystal thickness decreased. However, attempts to thin further than a rust-red colour by grinding inevitably led to crystals breaking up. Sufficiently robust crystals with an area adequate for spectroscopic measurements had a minimum thickness of around 10 μm. The second side, after the appropriate thinning, was then polished as the first. The thin sections were removed from the silica slide by placing in a bath of methanol for 12 h. These sections were subsequently handled using vacuum tweezers.

The final thickness of the urania crystals was found by two methods. First, the crystal was weighed to ± 0.01 mg and the area found by examining the crystal on a square grid and determining the outline under a microscope. The thickness was calculated using the theoretical density of UO_2 of 10 960 kg m^{-3}. Secondly, a micrometer screw gauge, accurate to 1 μm, was used. This latter was normally employed on fragments of crystal that broke off during handling. The two methods

gave results agreeing to within 5%. The specimens used ranged from 12 to 30 μm thick.

The more transparent single crystals of ceria did not require such thin sections. They were however ground and polished in essentially the same way as for UO_2. Thicknesses ranged from 0.8 to 0.3 mm.

2.2. Preparation of solid solutions and powders

Cerium–uranium dioxide solid solutions having the composition range 40–100% CeO_2 were prepared using a modification of the method of Hofmann and Höschele [7] for preparing $2CeO_2 \cdot UO_2$. Calculated quantities of cerium(III) nitrate and uranyl(IV) nitrate were dissolved in water and excess dilute ammonium hydroxide added with stirring. An immediate yellow precipitate was formed that changed slowly over an hour through green to dark blue. The supernatant liquid was removed by decantation and the precipitate washed five times with 1% aqueous ammonium nitrate to prevent peptisation. After filtering the precipitate was washed with acetone, then ether, and dried under vacuum at 100 °C.

The resulting product was green, due to partial oxidation of the U(IV) ions. The excess oxygen was removed by heating in a current of hydrogen for 4 h at 900 °C and cooling in the hydrogen atmosphere. The powder was now dark blue but on sudden exposure to air proved to be pyrophoric, producing a dark green product. However, if air was allowed to diffuse in slowly over a period of two days, the dark blue product lightened in colour and was then stable in air.

Several previous investigators [8–11] have shown that the precipitated product from aqueous solutions of cerium(III) and uranyl(VI) salts are solid solutions and that the precipitation is quantitative.

Oxygen-deficient cerium dioxide powder was prepared from powdered ceria, previously obtained by heating freshly precipitated cerium(III) hydroxide in air at 1000 °C. The pale yellow oxide was partially reduced by heating in hydrogen at temperatures between 500 and 900 °C for several hours to effect varying amounts of reduction. After cooling, part of the powder was reserved for diffuse reflectance measurements and stored in an inert gas dry-box. The remainder was transferred to a pre-weighed, well stoppered container. After weighing, reoxidising by heating in air, and reweighing, the degree of non-stoichiometry, and thus the value of x in CeO_{2-x}, was obtained.

2.3. Oxidation, reduction and annealing of crystals and powders

Crystals were treated in a silica tube, sealed at one end and mounted vertically. A crystal was placed in the tube and the top sealed with a silicone rubber stopper through which was fitted a chromel–alumel thermocouple and a silica capillary tube. These inserts ended about 5 mm above the crystal. The silica tube was positioned above a tube furnace which could be readily raised vertically, using a counter-balancing weights system. When the crystal was in the middle of the furnace hot zone the upper end of the silica tube protruded approximately 200 mm above the furnace. Oxidation reactions were performed in air, oxygen or gas mixtures of CO_2–CO, and reductions in hydrogen. The required gas was passed through the silica capillary tube and exited through a side-arm near the stopper (and through which back-diffusion was eliminated).

When treated in air or partial pressures of oxygen the gas was pre-dried over a molecular sieve. When hydrogen was used traces of oxygen were first removed, before drying, by passage over a platinum catalyst (Engelhard hydrogen purifier). The maximum temperature employed was 1000 °C. Crystals were also annealed by the above method except that a preheated furnace was used and the crystals were quenched by rapidly lowering the furnace.

Stoichiometric UO_2 was first obtained by heating the thin single crystal specimens in hydrogen or carbon monoxide at up to 1050 °C for several hours. Non-stoichiometric UO_{2+x}, of known x, was prepared by heating in various controlled partial pressures of oxygen, obtained by heating mixtures of CO_2–CO of defined CO_2/CO ratios at the appropriate temperature [1].

Powders and solid solutions were oxidised and reduced in a silica tube in a horizontal tube furnace, with the gas flowing over the powder. After reduction the sample was allowed to cool under hydrogen, and the ends of the tube sealed before transfer to an inert gas dry-box.

2.4. Crystal mounting devices

Since the polished crystals varied in size, several crystal holders were made. For the most robust ceria crystals the holder consisted of pairs of stainless steel caps, each of which contained a recessed hole fractionally deeper than the crystal thickness (Fig. 2). The single crystal section could thus be held in the optimum position over the hole but without applying pressure. The holders were then inserted into a stainless steel block attached to a stainless steel tube down which a gas could be passed (Fig. 3(a)). A thermocouple was located in a small hole in the block and the whole assembly fitted into a standard 10 mm silica optical cell on to which a long neck had been attached (Fig. 3(b)).

This system was used initially for the thin fragile urania crystals. These were not always of uniform thickness (avoiding a slight wedge during the final stages of hand-grinding and polishing is difficult) and in the vertical position, and during temperature changes, the

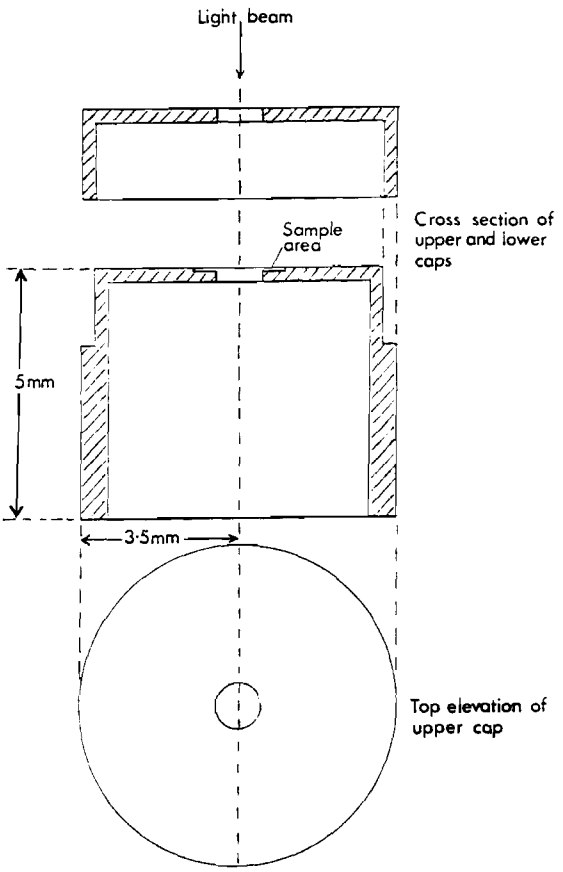

Fig. 2. Stainless steel holder for single crystals of ceria.

caps would sometimes separate slightly and the crystal move so that it was no longer covering the aperture. For these crystals the holder shown in Fig. 4 was successfully employed. The procedure was that a crystal was first placed on plate C so that it completely covered the aperture (about 4 mm^2). Plate D, fractionally thicker than the crystal was then placed over the crystal and in alignment with C. A hole had previously been cut in D to fit loosely over the crystal lying in its optimum position on C. The cover plate E was then screwed down tightly over D to contain securely, but not compress, the thin fragile crystal. When located vertically the crystal did not move. To reduce metal scaling at high temperatures the block and plate were now made of pure nickel.

Some urania crystals, after grinding and polishing, were considered too delicate to be removed from the microscope slides and placed in the crystal holder. Their spectra could however be taken at room temperature while still attached to the slide after areas of the slide and crystal had been masked off with an appropriate plate C.

2.5. Spectroscopic measurements and relationships

An Applied Physics Cary 14H research spectrophotometer, fitted with a digitising attachment, was used.

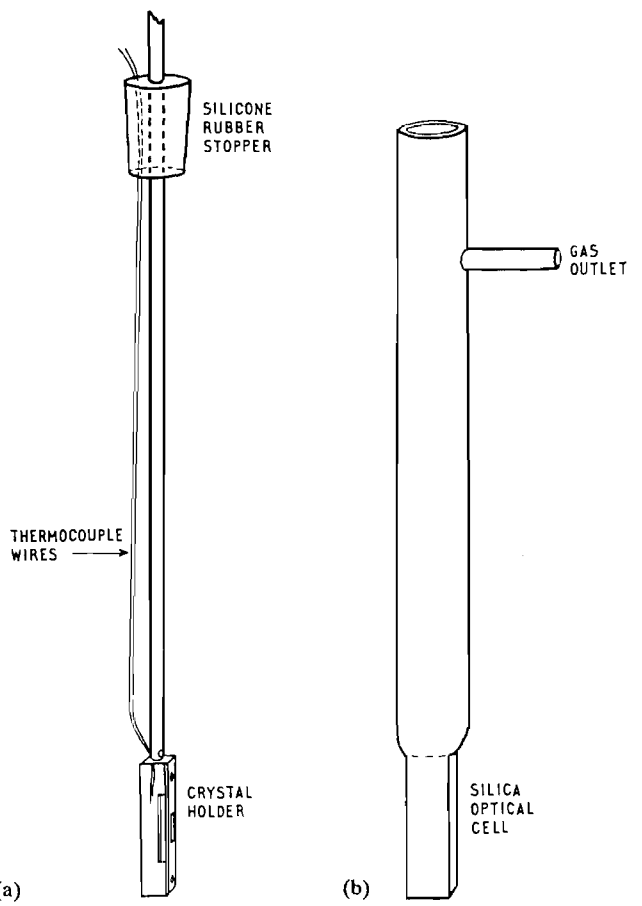

Fig. 3. (a) Stainless steel block for the crystal mounting device in Fig. 2. (b) Extended silica optical cell in which block (a) is placed, and the whole assembly placed in a furnace and the required gas passed slowly over the crystal.

This instrument, in the rare H (high temperature) mode, has a large sample compartment and permits accurate spectra to be recorded at temperatures in excess of 1000 °C and up to absorbance readings approaching 6. Details have been given elsewhere [12,13] regarding the spectrophotometer, computer treatment of spectra and the various furnaces employed. Diffuse reflectance spectra measurements were made using a Unicam SP700 recording spectrophotometer. The standard specimen holder of the diffuse reflectance attachment was replaced by one in which stoppered circular 2 mm path length silica cells were used to contain the samples. The sample powders could thus be loaded under nitrogen and diffuse reflectance spectra obtained of oxygen sensitive materials. The reference material was a fresh circle of filter paper. Previous experiments had shown filter paper to be indistinguishable from the recommended standard of freshly prepared magnesium oxide over the spectral range of interest, and considerably more convenient.

For absorption spectra the following relationships apply. The absorbance, A, is given by $\log(I_0/I)$, where

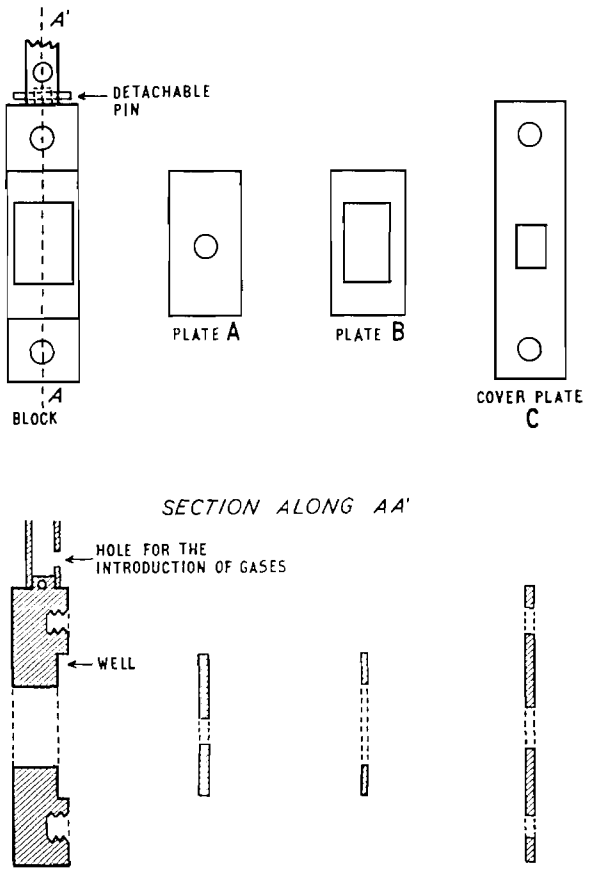

Fig. 4. Nickel holder for ultra-thin wafers of single-crystal urania.

I_0 is the intensity of the incident light and I is the transmitted intensity. For a crystal the absorption coefficient, α (usually expressed in cm^{-1}), is given by $\alpha = A/d$, where d is the crystal thickness. The units of the electromagnetic spectrum, on the commonly preferred energy scale of wavenumber, are also expressed in units of cm^{-1}. To avoid possible confusion the alternative frequency units of kilokayser (kK) will be at times employed, where 1 kK = 1000 cm^{-1}. For conversion to electron volts, 1 kK = 0.12398 eV. Since all spectra were recorded on spectrophotometers calibrated linearly in reciprocal energies, i.e. wavelength (nm), these units will be included, particularly where authoritative data are needed.

3. Results and discussion

3.1. Electron transfer in ceria

3.1.1. Effect of non-stoichiometry upon absorption spectra of ceria

3.1.1.1. Single crystal ceria

Single crystals of cerium dioxide were heated in hydrogen to reduce ceria to the non-stoichiometric CeO_{2-x}. Heating at temperatures below 480 °C had no observable effect but above this temperature the crystals became blue, the intensity increasing with increasing temperature. Above 600 °C the crystals became opaque. The absorption spectra of the blue crystals were made after cooling to room temperature, and still in a hydrogen atmosphere. The crystals were then exposed to air at room temperature and their spectra re-recorded at regular intervals for several weeks. The absorption did not change. The lightly coloured crystals showed the formation of a broad absorption band centred around 12 500 cm^{-1} (1.550 eV) but as higher temperatures of reduction were used it shifted to 15 140 cm^{-1} (1.887 eV), Fig. 5. The coloration could be reversed and removed by heating in air, and the original spectrum of each now colourless crystal was then reproduced.

To determine if the blue colour occurred homogeneously throughout the crystal, or if it was a surface effect, a crystal was ground and polished, and its spectrum retaken several times. The measured absorbance at the band maxima and selected wavelengths were directly proportional to the crystal thickness, thus indicating homogeneity.

Attempts were made to determine x in CeO_{2-x} by weighing crystals before and after reduction and again after reoxidation. A microbalance capable of measuring a weight change of 0.005% was used but no measurable weight change was found, thus indicating that in the most intensely coloured crystal x was less than 0.0005.

3.1.1.2. Powdered ceria

Pale yellow cerium dioxide powder was reduced in hydrogen above 500 °C to a blue coloration. Upon exposure to air at room temperature it reverted almost instantaneously to the pale yellow powder with considerable heat evolution. Fig. 6 shows the diffuse reflectance spectra of powdered cerium dioxide under

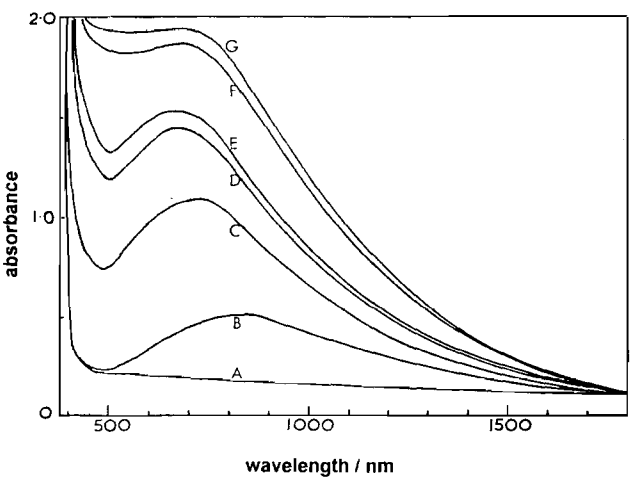

Fig. 5. Absorption spectra of single-crystal CeO_2 after reduction in hydrogen. A, reduction temperature <480 °C; B, 485 °C; C, 512 °C; D, 520 °C; E, 526 °C; F, 535 °C; G, 540 °C.

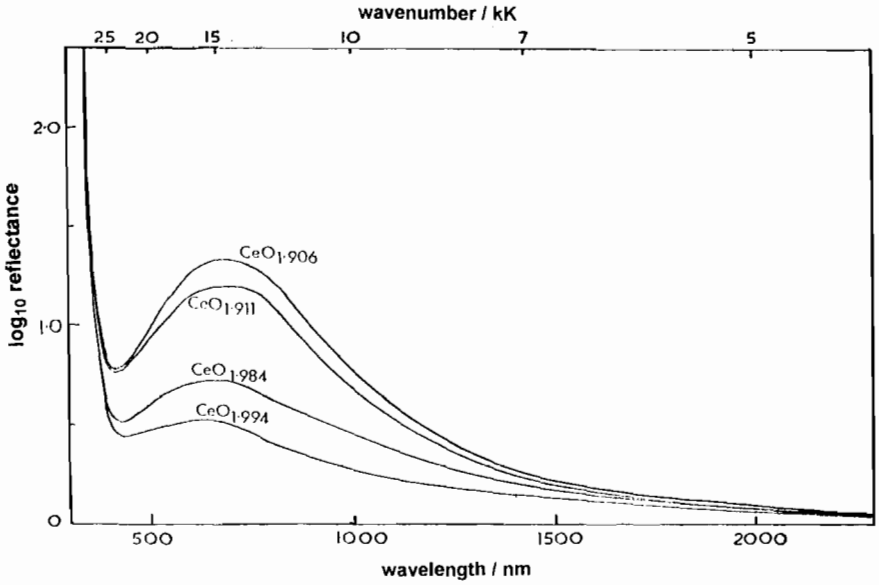

Fig. 6. Diffuse reflectance spectra showing the effect of increased reduction of ceria powder.

hydrogen, having been reduced at various temperatures in the range 500 to 900 °C. All show a broad absorption band centred around 14 900 cm^{-1} (1.847 eV).

The stoichiometry of the reduced samples were determined from the weight increase on reoxidation and gave values in the range $CeO_{2.000}$ to $CeO_{1.900}$.

The absorption bands found in both reduced single crystal and reduced powdered ceria (Figs. 5 and 6) are similar, but only single crystals that had been reduced below 500 °C showed the band maxima at 12 500 cm^{-1} (1.550 eV).

3.1.2. Electron transfer between Ce^{3+} and Ce^{4+}

The blue colour of reduced cerium dioxide has been suggested [2,3] as arising from electron transfer between Ce^{3+} and Ce^{4+} ions, but its absorption spectrum has not previously been reported. The anion vacancy in CeO_{2-x} has clearly been identified as the defect responsible for hypo-stoichiometry and oxygen transport [14–16]. It is interesting to note that when aqueous ammonia is added to an aqueous solution of either a cerium(III) or a cerium(IV) salt, a white precipitate of cerium(III) hydroxide or a pale yellow precipitate of hydrated cerium(IV) oxide, respectively, is formed. However, if the aqueous ammonia is added to a solution containing both cerium(III) and cerium(IV), a dark blue precipitate is rapidly formed.

Deviation from the stoichiometric composition, $CeO_{2.000}$, results in a deeper coloration in the single crystals than with powdered samples. This is attributed to the shorter optical path length involved in the diffuse reflectance measurements, compared with the transmission path length through the single crystals.

The defect structure of the fluorite lattice and the cerium–oxygen system has been investigated. The solubility of rare earth sesquioxides in the fluorite lattice, e.g. CeO_2–La_2O_3 [17], has been found to be large [18], from about 20 to 40 mol%. Indeed, the cerium–oxygen system can be regarded as a problem concerning the miscibility of Ce_2O_3 in CeO_2. However, for this system Bevan [18] found that the composition range of the single fluorite phase was very small, and appreciable reduction led to the formation of other phases. Thus an important difference between the binary system Ce(IV)–Ce(III)–O_2 and the binary system Ce(IV)–rare-earth(III)–O_2 is the composition range of the fluorite phases. In the former system it is very small, yet in the latter system it is large. Bevan [18] suggested that this difference in behaviour was due to the formation of metastable states in the Ce(IV)–rare-earth(III)–O_2 system.

The usual method of preparation of these systems was to co-precipitate the hydroxides from a mixture of the solutions of the nitrates. This method results in a high degree of dispersion of the cations, and which is retained on conversion to the oxide, and thus a truly mixed crystal. The structure of the crystal, however, depends upon the capacity of the separate oxide structures to nucleate with a sufficient degree of distortion. Over a wide composition range, the fluorite phase is preferred. It is therefore possible that the mixed crystals formed by this method are metastable with respect to the separate oxide phases. The attainment of equilibrium necessitates the rearrangement of the cation lattice, but the mobility of cations in the fluorite lattice is very low. However, in the Ce(IV)–Ce(III)–O_2 system, the cation rearrangement can occur by 'electron switching' between Ce^{3+} and Ce^{4+}, and hence a cation diffusion process is not needed in this case.

The above thus shows that the concept of electron transfer between Ce^{3+} and Ce^{4+} ions in the cerium–oxygen system can be used to explain not only the deep colour of the non-stoichiometric oxide [2,3] but also the formation of new phases within this system.

3.1.3. Effect of impurities on the absorption spectrum of cerium dioxide

Three types of crystal were available. All contained a small amount of tungsten(VI) and some had in addition either neodymium(III) or dysprosium(III) in concentration about ten times that of the tungsten impurity. However, the tungsten-only crystals were pale blue and the rare earth doped ones were colourless. Spectra are compared in Fig. 7. The blue colour corresponds to a very broad band centred around 12 500 cm^{-1} (1.550 eV). This band is at the same position and very similar in intensity and shape to that obtained when pure ceria crystals were reduced at 480 °C (Fig. 5). The band in the tungsten-doped crystals can thus be explained as arising from the same type of electron transfer transition occurring in non-stoichiometric cerium dioxide, namely electron transfer between Ce^{3+} and Ce^{4+} ions. The presence of Ce^{3+} ions in these crystals would compensate for the 'excess' positive charge of the W^{6+} ion compared with the host Ce^{4+} ions. Hence the blue coloration, and band, cannot be removed by heating in air, as with oxygen-deficient cerium dioxide. The more heavily doped crystals are colourless because the Nd^{3+} or Dy^{3+} ions compensate completely for the W^{6+} ions. No Ce^{3+} ions need therefore be present for charge compensation and hence no bands due to intervalence transitions are observed.

This explanation is in accord with the measurements of Linares [19] on pure cerium dioxide, doped with F^-, Nb^{5+} and Ta^{5+}. All these doped crystals were blue, but this coloration was attributed, in a general way, to colour centres. As now expected, the blue coloration did not occur if the doped crystals also contained trivalent rare earth ions. No absorption spectra of the blue crystals were reported, but a band essentially the same as that in Fig. 5 is expected, due to electron transfer between Ce^{3+} and Ce^{4+} ions. The Nb^{5+} and Ta^{5+} ions will behave in an analogous manner to the W^{6+} impurity in the present work, so that Ce^{3+} ions are present for charge compensation. The presence of F^- at oxygen sites represents a lack of negative charge, which would also be compensated by the presence of Ce^{3+} ions, again giving rise to intervalence spectra. The effect of the trivalent rare-earths observed by Linares [19] is identical to the charge compensating effect of the Nd^{3+} and Dy^{3+} ions described here.

The increased darkening of these crystals at higher temperature under hydrogen, compared with the tungsten-only doped crystals, is in agreement with the findings of Brauer and Holdsmidt [20]. They observed that the reduction of cerium dioxide in hydrogen could be accelerated by the presence of certain impurities. They showed that the addition of U(IV), Pr(III), Tb(III) and many other trivalent rare-earths all facilitated reduction. In the last example, they explained the effect as the easier migration of the O^{2-} ion to the crystal surface due to the presence of the greatly increased number of oxygen vacancies in the impure oxide. Thus the crystals doped with Dy^{3+} and Nd^{3+} in the present work would be expected to be reduced further, and hence more deeply coloured, than pure ceria crystals when reduced at the same temperature for the same length of time before quenching.

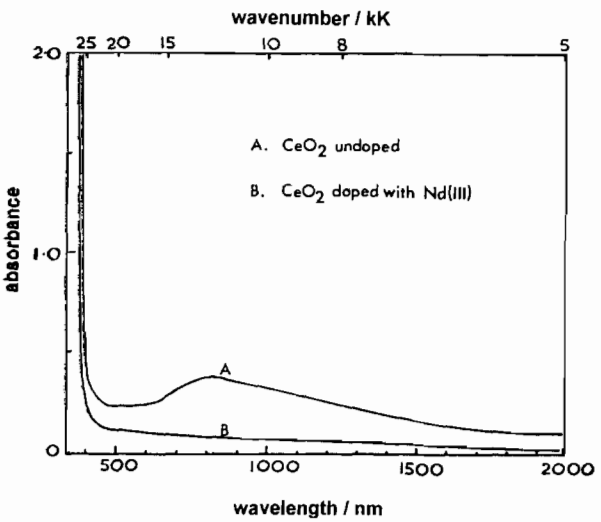

Fig. 7. Effect on the absorption spectra of single-crystal CeO_2 of doping with the rare-earth oxide Nd_2O_3.

3.1.4. Electrical conductivity of cerium dioxide

A consequence expected of intervalence absorption spectra would be that the electrical conductivity of reduced samples would be greater than that of the stoichiometric oxide. D.c. electrical conductivity measurements of single crystals of pure ceria, before and after reduction, showed that the conductivity increased by a factor of around 10^3 after heating in hydrogen between 500 and 550 °C. The work reported concerning the electrical conductivity of cerium dioxide has all been concerned with compressed powders or sintered material. According to Croatto [21], ionic conduction occurs in the mixed oxide system CeO_2–La_2O_3. The presence of the impurity cation of oxidation state less than +4 results in formation of anion vacancies and contributes to the conductivity effectively by migration of these defects under the influence of an applied electric field.

Honig and Czanderna [22] made d.c. measurements of the electrical conductivity of ceria in the temperature range 160–485 °C under vacuum. A reversible oxygen loss was noted, together with an increase in electrical

conductivity of four orders of magnitude over this temperature range. They also found that the oxide was stable from 485 to 600 °C, above which more oxygen was lost. They suggested that the electrical conductivity increase in the lower temperature range was due to loss of oxygen from the surface of the material, and that this was responsible for the conductivity change. Later Rudolph [23] showed that cerium dioxide was an n-type semiconductor above 850 °C. This was more recently confirmed by Tuller and Nowick [24] who noted exceptionally large oxygen vacancy densities at the fluorite phase limit [25] ($x \sim 0.3$ for CeO_{2-x} at 1000 °C). Doubly and singly ionised oxygen vacancies dominate the equilibria and function as donor centres, with the former dominating at smaller values of x [24], the conditions experienced here. Conductivity increased at higher temperatures and Noddack and Walch [26] found that the conduction mechanism was essentially electronic in the range 600 to 1300 °C. They could not detect any liberated oxygen in their experiments and concluded that the ionic contribution to the electrical conductivity was less than one part in 500.

Kevane et al. [27] made d.c. measurements at 460 °C on cerium dioxide doped with Ca^{2+} at various concentrations. Conductivity increased with increasing calcium content, and a blue coloration was formed in the oxide, initially at the cathode and which grew towards the anode. The current initially increased rapidly and then levelled off. These results were explained as an ionic conduction process with migration of oxygen towards the anode, and the blue coloration as oxygen deficiency. The blue material formed had a lattice constant slightly larger than the starting material, as is expected for the oxygen deficient oxide.

Most of the work on the electrical conductivity of cerium dioxide was made prior to the electron hopping theory of Heikes and Johnston [28]. Thus no interpretation of the electronic conduction of oxygen deficient ceria has been made in terms of the electron hopping theory. However there is no difficulty in applying this theory rather than band theory to account for the electrical conduction of partially reduced cerium dioxide, particularly since both approaches have been applied to uranium dioxide. Thus for the present work, the increase in conductivity can be attributed to electron hopping from Ce^{3+} to Ce^{4+} ions or the presence of Ce^{3+} donor levels in the forbidden energy gap.

The thermal energy gap in cerium dioxide is 8850 cm^{-1} (1.097 eV) and the optical value, from the fundamental absorption edge is seen at 26 000 cm^{-1} (3.223 eV) in Fig. 8. This is the energy required to excite an electron across the band gap. Immediately after the electron transition, the ions surrounding the atom from which the electron was removed will no longer be in equilibrium and hence they will move to new lower energy equilibrium positions. The thermal energy required to lift the electron from its valence energy level to the conduction band is only that required to raise it into the conduction band with the ions in equilibrium positions. Thus the optical activation energy is always greater than the thermal activation energy for ionic materials.

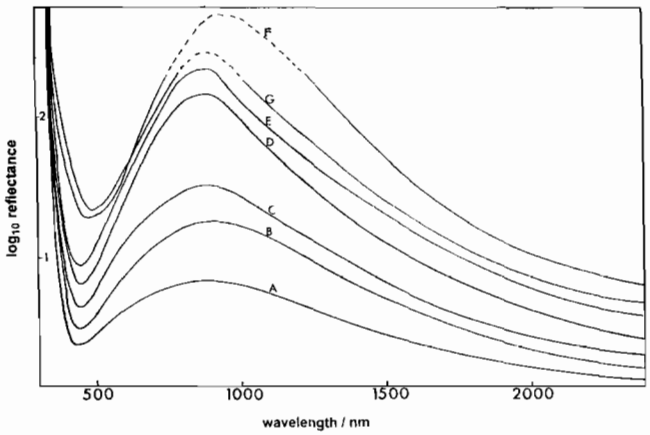

Fig. 8. Diffuse reflectance spectra of cerium dioxide–uranium dioxide solid solutions. A, mol% CeO_2, 99: mol% UO_2, 1; B, 95:5; C, 90:10; D, 80:20; E, 66.6:33.4; F, 50:50; G, 40:60.

3.2. Electron transfer in solid solutions of cerium dioxide and uranium dioxide

The diffuse reflectance spectra of all solid solutions of cerium dioxide and uranium dioxide showed a broad intense band at 11 100 cm^{-1} (1.376 eV) over the composition range 1–60 mol% UO_2 (Fig. 8). Reflectivities < 0.5% are of less accuracy and are represented in the figure by dashed lines. Hofmann and Höschele [7] attributed the blue coloration of the oxide of composition $2CeO_2 \cdot UO_2$ to an 'oscillation of valency', arising from

$$Ce_2(IV)U(IV)O_6 \longleftrightarrow Ce_2(III)U(VI)O_6 \quad (5)$$

Robin and Day [2], in their discussion of mixed valence transitions in these solids, stated that the colour was a maximum around the 2:1 mole ration of CeO_2:UO_2, quoting as their source Brauer and Tiessler [8]. This implies that the intervalence transition is of the form proposed by Hofmann and Höschele [7]. However Brauer and Tiessler [8] reported that the colour of the solid solutions became darker as the percentage of uranium dioxide was increased. This corresponds with our diffuse reflectance spectra. Spectrum E in Fig. 8 shows the same 2:1 mol ratio, and although the spectra of the solid solutions containing large UO_2 proportions are less accurately defined around the band maximum there is no diminution of band intensity. Electrical conductivity measurements showed a maximum for the solid solution containing 35 mol% cerium dioxide. There

is therefore no evidence to indicate that intervalence transfer occurs to the maximum extent in the composition $2CeO_2 \cdot UO_2$.

In the present work, the most intensely absorbing solid solution was obtained with an equimolar mixture of the oxides. It is important to note that the solid solution containing 60 mol% UO_2 absorbed less at energies below 15 400 cm^{-1} (1.909 eV) than the 50:50 mixture, Fig. 7. If there was a significant contribution to the absorption by the presence of UO_2 alone, then this contribution would be greater in the solid solution containing 60 mol% urania than in the equimolar mixture. Since the latter absorbed more strongly in this region there is no doubt that the intervalence absorption was greatest in the 50:50 mixture. This indicates that the electron transfer is of the form

$$Ce(IV) + U(IV) \longrightarrow Ce(III) + U(V) \quad (6)$$

3.3. Electron transfer in single crystal urania

3.3.1. Absorption spectrum of non-stoichiometric UO_{2+x}

The study of intervalence transitions in the uranium–oxygen system is very much more complicated than for ceria. Firstly uranium is normally found in the U^{4+}, U^{5+} and U^{6+} oxidation states and compounds involving these, viz. UO_2, U_4O_9, U_3O_7, U_3O_8 and UO_3, are well known. Secondly the visible and near-IR spectrum of stoichiometric UO_2 is already complicated by numerous narrow bands superimposed on a sharply rising absorption edge commencing at ~16 000 cm^{-1} (2 eV), right in the middle of the range expected in the study of any intervalence bands.

Fig. 9 shows a set of absorption spectra, measured at ambient temperature, for stoichiometric UO_2 and for non-stoichiometric UO_{2+x} for various small values of x, obtained after controlled oxidation at high temperatures (750–1050 °C) in CO–CO_2 mixtures at appropriate fixed ratios, followed by quenching to room temperature. There is a general increase in absorbance with an increase in x. The spectral changes resulting are more clearly seen by subtracting the base spectrum for stoichiometric UO_{2+x} and comparing the difference spectra (Fig. 10). Four main changes are apparent with x increase, namely, (i) a shift in the sharply rising absorption edge, which commences at 17 750 cm^{-1} (2.2 eV), to higher energy; (ii) an overall decrease in the intensity of the numerous small narrow $U^{4+}(5f^2)$ intracationic transitions; (iii) a small peak appears at 6300 cm^{-1} (0.78 eV) which increased with increasing x; and (iv) a very broad band appears with a possible maximum around 16 000 cm^{-1} (2 eV), near the onset of the absorption edge.

The absorption edge belongs to a band of maximum absorption coefficient of ~120 000 cm^{-1} at a peak position of around 25 800 cm^{-1} (3.2 eV). This band is due to the transition $5f^2 \rightarrow 5f^16d(e_g)$, and its low energy edge shifts to higher energy with increasing x.

Most of the structure seen in the spectrum of UO_2 between 4000 and 17 750 cm^{-1} (0.5 and 2.2 eV) is due to phonon-assisted intracationic transitions $U^{4+}(5f^2) \rightarrow U^{4+}(5f^2)$. The incorporation of interstitial oxygen into the lattice, oxidises some U^{4+} ions to U^{5+} and U^{6+}. The diminished U^{4+} concentration shows up as a trough in the difference spectrum, particularly in the region of the more intense f–f transitions around 14 500 cm^{-1} (1.8 eV).

The emerging small peak at 6300 cm^{-1} (0.78 eV), which is also observed in the spectra of UO_{2+x} at 304 °C, is due to the transition

$$U^{5+}(5f)^2F_{5/2} \longrightarrow U^{5+}(5f)^2F_{7/2} \quad (7)$$

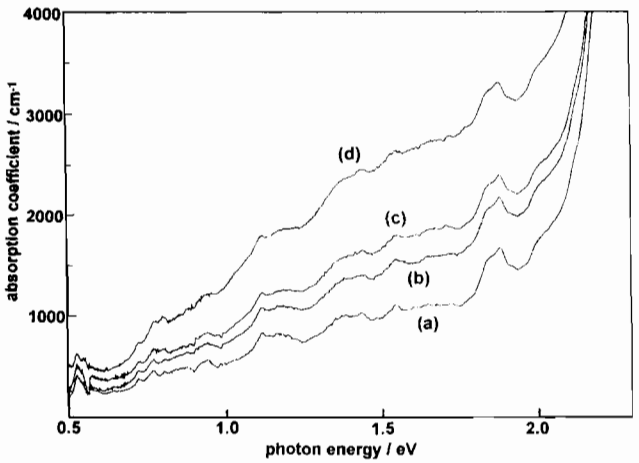

Fig. 9. Absorption spectra at room temperature of UO_{2+x} for $x=0$ (a), 0.035 (b), 0.041 (c), 0.059 (d).

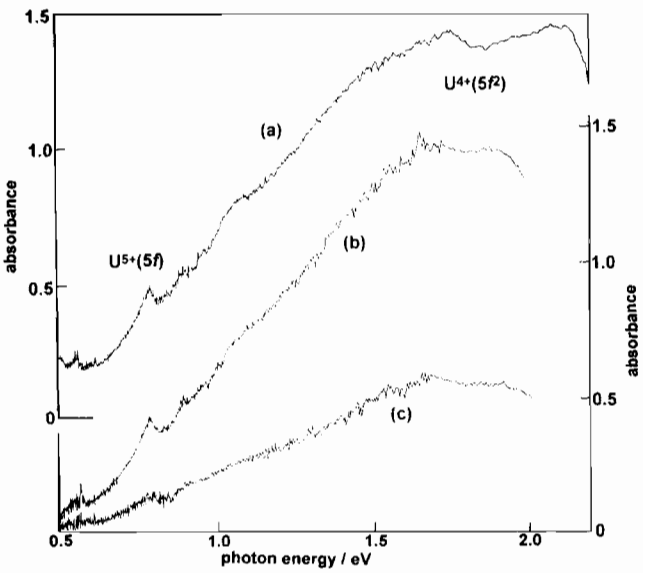

Fig. 10. Difference spectra between UO_{2+x} and UO_2 showing the absorption profile due to the excess of oxygen: (a) for $x=0.059$ at 24 °C; (b) $x=0.059$ at 304 °C; (c) $x=0.037$ at 304 °C. Note the appearance of the $U^{5+}(5f)$ band and the effect of the consequent decreasing concentration of U^{4+} and its ($5f^2$) band.

The narrow width of 320 cm^{-1} (0.04 eV) at 20 °C broadening to 565 cm^{-1} (0.07 eV) at 304 °C is comparable with the widths of the $U^{4+}(5f^2)$ intracationic transitions. This peak is not present in stoichiometric UO_2 but has been observed in the spectra of U_3O_8 and $(U,Th)O_{2+x}$, both of which are materials in which concentrations of U^{5+} are expected [29].

3.3.2. Intervalence transitions in UO_{2+x}

The main change in the spectra of UO_2 and UO_{2+x} as oxidation proceeds is the appearance and growth of a very broad band commencing at about 4000 cm^{-1} (0.5 eV) and peaking at around 16 000 cm^{-1} (2 eV). This band is attributed to intervalence transitions involving the transfer of a single localised f electron between adjacent uranium ions in various oxidation states, typically of the form

$$U^{4+}(5f^2)+U^{5+}(5f) \longrightarrow U^{5+}(5f)+U^{4+}(5f^2) \quad (8)$$

The presence of intervalence bands is expected in non-stoichiometric UO_{2+x} as there is clearly the possibility of electron transfer between adjacent oxidised cations; and the appearance of such bands is often accompanied with changes in electrical conductivity.

In hyper-stoichiometric UO_{2+x}, electrical conduction occurs by a mechanism of hole hopping from U^{5+} to U^{4+} and the values of the activation energy, E_t, have variously ranged from 1370 to 2740 cm^{-1} (0.17 to 0.34 eV). If at high temperature the activation and optical energies, E_t and E_a, are directly related on the basis of a simple symmetrical intervalence process, an absorption band is expected to peak in the region 5500 to 11 000 cm^{-1} (0.68 to 1.36 eV).

Assuming that this band is due to a single intervalence process it was fitted, using a computer program, to a Gaussian profile. Spectra recorded at 20 and 304 °C for various values of x were resolved and the minimised peak positions, bandwidths at half height and absorption coefficients obtained are summarised in Table 1. Fig. 11 illustrates the band resulting from subtracting the spectrum of UO_2 from that of UO_{2+x}, where x is 0.059, together with the best fit of a Gaussian-shaped band.

Table 1
Gaussian band parameters computed for the intervalence band in the spectrum of UO_{2+x} at room and elevated temperatures

Temp. (K)	x	Absorption coefficient (cm^{-1})	Position (eV)	fwhh[a] (eV)
297	0.035	528	1.80	1.39
297	0.041	720	1.79	1.33
297	0.059	1847	1.86	1.69
577	0.037	696	1.79	1.28
577	0.059	1835	1.75	1.28

[a]fwhh = full bandwidth at half peak height.

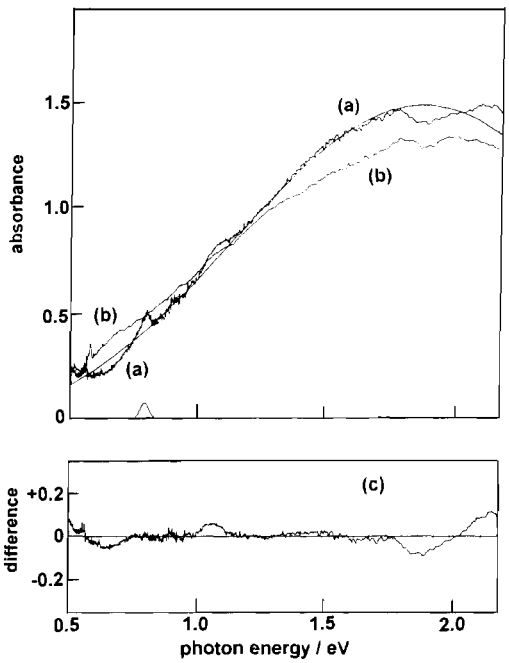

Fig. 11. (a) Difference spectrum for UO_{2+x}, where $x=0.059$, at 24 °C and the best fit to a Gaussian curve. (b) Difference profile recorded after several weeks at ambient temperature. Note decrease in intensity of the $U^{5+}(f)$ band and consequent reduced decrease in the $U^{4+}(5f^2)$ feature compared with (a), the fresh sample. (c) Difference between intervalence band and Gaussian curve.

However, although it is possible to fit the main broad absorption profile to a single Gaussian band, there remain serious problems associated with this type of fitting. Because the band has a maximum near the absorption edge and irregular structure around 15 300 cm^{-1} (1.9 eV), less than half of the profile can be used for fitting to a Gaussian band. Table 1 shows that when difference profiles, as in Fig. 11, are resolved into a single Gaussian band the peak positions centre around 14 500 cm^{-1} (1.8 eV) and with a half-width of at least 9700 cm^{-1} (1.2 eV).

3.3.3. Longer term changes in the spectrum of UO_{2+x}

It has been observed that spectra taken some weeks or months after the initial oxidation studies show subtly different forms to those of the freshly oxidised samples described above. The changes observed over a long period are: (i) a small shift in the absorption edge to lower energies; (ii) a definite decline leading to extinction of the $U^{5+}(5f)$ peak at 6300 cm^{-1} (0.78 eV); (iii) a subtle change in the shape of the main broad intervalence band with a small increase in the absorbance at lower energies which appears to generally broaden this band, Fig. 11. It has not been possible to monitor any changes in the small narrow $U^{4+}(5f^2)$ intracationic transitions.

3.3.4. Effect of increase in x in UO_{2+x} on cluster formation and electron transfer

The increase in overall increase in absorbance in the visible region of the spectrum, due principally to a very broad band centred at 14 500 cm^{-1} (1.8 eV), is consistent with spectra for thin films of UO_{2+x} for various x ($0 < x < 0.25$) reported by Ackermann et al. [30], which also suggests a very broad band with a possible maximum approaching 16 000 cm^{-1} (2 eV). This band is also comparable with the symmetrical intervalence transition between Ce^{4+} and Ce^{3+} in ceria (Fig. 5) which also has a maximum at about 14 500 cm^{-1} (1.8 eV). An initial explanation for the origin of this band in UO_{2+x} suggests a simple symmetric intervalence transition of the form given by Eq. (8) with no overall energy change, E_o, consistent with the comparatively low energy of the band. However the width of this band, from 9700 to 13 700 cm^{-1} (1.2 to 1.7 eV), is far larger than would be expected on the basis of a single intervalence transition; and the subtle changes in shape that are observed over a long period of time do suggest that this band is not due to a single intervalence process. We therefore consider that the observed profile is more likely to consist of an envelope of several intervalence transitions between cations in sites variously associated with clusters involving interstitial oxygen.

It is often useful to consider the oxidation of UO_{2+x} for $x < 0.25$ on the basis of the two types of clusters first identified by Willis [31], in which the excess oxygen is incorporated in interstitial sites, initially in 2:1:2 clusters and as x is increased 2:2:2 clusters are formed. Allen and Tempest [32] have suggested that the latter may subsequent be formed in cluster chains. For both clusters the presence of the interstitial oxygen displaces some of the lattice oxygen. Although the cation lattice remains fixed in position, the anion environment surrounding many of the uranium ions is variously changed.

Hitherto [1,33,34] it has been assumed that because the apparent position of the intervalence band(s) lies at a low energy of below 16 000 cm^{-1} (2 eV), the intervalence band observed is most likely to be between symmetrical or nearly symmetrical intervalence transitions of the type given by Eq. (8) such that the overall energy change E_o is zero or quite small. Because the anion environment of many of the cations is altered, a multitude of intervalence transitions are possible, each with a particular energy and associated half-width and intensity dependent on the concentrations of the initial and final states. The observed spectrum is thus a broad envelope consisting of many transitions commencing at ~4000 cm^{-1} (0.5 eV) and extending to higher energy.

More recent measurements indicate that while the presence of the U^{5+} cation as revealed by the peak at 6300 cm^{-1} (0.78 eV) is clearly demonstrated in freshly oxidised samples quenched from controlled oxidation at high temperatures, the decrease of this peak in samples left at ambient temperatures and the only slight shift in the shape of the main broad band that accompanies the decrease in this U^{5+} peak, does now raise the possibility that intervalence transitions involving the U^{5+} ion may not be the main contributor to the intervalence spectrum of UO_{2+x} and that this band which is brought on by the oxidation of UO_2 is principally due to intervalence transitions involving U^{6+} cations

$$U^{4+} + U^{6+} \longrightarrow U^{5+} + U^{5+} \quad (9)$$

It was hitherto assumed that because the cations states were so different, the overall energy change E_o, for this transition would be high and the corresponding optical transition would not be seen below 16 000 cm^{-1} (2 eV); it seems now that this energy may be quite small. The persistence of the U^{5+}(5f) peak at ambient temperatures after quenching from the UO_{2+x} region (above about 450 °C for $x = 0.06$) indicates that the energy of the metastable U^{5+} associated with an interstitial cluster is only slightly higher than when oxidised to U^{6+} and associated with some form of defect aggregate.

Since quenching from high temperature is never instantaneous, the observed spectrum will consist of contributions from both types of intervalence transitions, Eqs. (7) and (8). A careful comparison of the spectra of UO_{2+x} taken immediately after quenching with that taken several weeks later, Fig. 9, does suggest the presence of a narrower intervalence peak at about 14 500 cm^{-1} (1.8 eV) with a half-width of about 5650 cm^{-1} (0.7 eV). This is also superimposed on the underlying broader band produced by transitions of the type in Eq. (9) involving U^{6+} in defect aggregates. The narrower band has a half-width more compatible with that for the symmetrical intervalence transition of Eq. (8) [34].

The precipitation out of the U^{5+} ions at ambient temperatures and the formation and growth of defect aggregates (possibly involving U^{6+}) is confirmed by X-ray diffraction (XRD) measurements made on a sample of single crystal $UO_{2.059}$. The observed lattice spacings of 547.0 and 539.3 pm are very close to the unit cell values of $a = 547.2$ and $c = 539.7$ pm for α-U_3O_7($UO_{2.33}$) with tetragonal structure [35,36]. The spacing at 547.0 pm coincides with the lattice parameter of UO_2 and masks any contribution from the underlying UO_2 substrate, thereby making estimates of the surface layer thickness difficult. If the peak at 6300 cm^{-1} (0.78 eV) is taken as a marker for U^{5+} in the uranium–oxygen system then we should conclude, from the absence of this peak in the near-IR region of the spectrum of this specimen taken prior to the XRD measurement, that U_3O_7 contains U^{4+} and U^{6+} but no U^{5+}.

Thus U^{5+} formed by oxidising at high temperatures in the UO_{2+x} phase can be 'frozen-in' by quenching to ambient temperatures and the intervalence transition

$$U^{4+} + U^{5+} \longrightarrow U^{5+} + U^{4+} \quad (10)$$

contributes to the spectrum of UO_{2+x} around 14 500 cm^{-1} (1.8 eV). These interstitial clusters precipitate slowly out of the matrix to form aggregates involving U^{6+}. These in turn accumulate and grow as U_3O_7 on surfaces and at grain boundaries etc. The main contribution to the increase in absorption with x is then due to the intervalence transition $U^{4+} + U^{6+} \rightarrow U^{5+} + U^{5+}$.

We therefore conclude that, after careful subtraction of the f–f transition spectra to reveal the intervalence spectra in UO^{2+x}, we have established that the fluorite lattice oxides CeO_{2-x} and UO_{2+x} do exhibit similar behaviour. Intervalence bands are observed in the visible region and in both systems electron transfer between cations in different oxidation states can bring about precipitation into two phases, leading in the case of urania to the formation of aggregates.

Acknowledgements

We thank Professor G.C. Allen, Dr P.A. Tempest and N. Holmes at Berkeley Nuclear Laboratories, Berkeley, Gloucestershire, for XRD measurements and helpful discussions. We also thank Dr P. Spencer, Leeds University, for the d.c. electrical conductivity measurements on single crystals.

References

[1] H.V.St.A. Hubbard and T.R. Griffiths, *J. Chem. Soc., Faraday Trans. 2, 83* (1987) 1215.
[2] M.B. Robin and P. Day, *Adv. Inorg. Chem. Radiochem., 10* (1967) 247.
[3] G.C. Allen and N.S. Hush, *Prog. Inorg. Chem., 8* (1967) 357.
[4] W.T. Doyle, *Phys. Rev., 111* (1958) 1072.
[5] N.S. Hush, *Trans. Faraday Soc., 57* (1976) 447.
[6] T.R. Griffiths and J. Dixon, *J. Chem. Soc., Faraday Trans., 88* (1992) 3475.
[7] K.A. Hofmann and K. Höschele, *Ber. Dtsch. Chem. Ges., 48* (1915) 20.
[8] G. Brauer and R. Tiessler, *Z. Anorg. Allg. Chem., 27* (1953) 273.
[9] W. Rüdorff and G. Valet, *Z. Anorg. Allg. Chem., 271* (1953) 257.
[10] W. Rüdorff and G. Valet, *Z. Naturforsch., Teil B, 7* (1952) 57.
[11] A. Magneli and L. Kihlbor, *Acta Chem. Scand., 5* (1951) 578.
[12] T.R. Griffiths and P.J. Potts, *J. Chem. Soc., Dalton Trans.,* (1975) 344.
[13] H.V.St.A. Hubbard, *Ph.D. Thesis,* Leeds University, UK, 1981.
[14] B.C.H. Steele and J.M. Floyd, *Proc. Br. Ceram. Soc., 19* (1971) 55.
[15] J.M. Floyd, *Indian J. Technol., 11* (1973) 589.
[16] G.E. Murch and C.R.A. Catlow, *J. Chem. Soc., Faraday Trans., 2, 83* (1987) 1157.
[17] E. Zintl and U. Croatto, *Z. Anorg. Chem., 242* (1939) 79.
[18] D.J.M. Bevan, *J. Inorg. Nucl. Chem., 4* (1955) 1.
[19] R.C. Linares, *J. Phys. Chem. Solids, 28* (1967) 1285.
[20] G. Brauer and U. Holtschmidt, *Z. Anorg. Allg. Chem., 279* (1955) 129.
[21] U. Croatto, *Ric. Sci., 13* (1942) 830.
[22] J.M. Honig and A.W. Czanderna, *Phys. Chem. Solids, 6* (1958) 96.
[23] J. Rudolph, *Z. Naturfursch., Teil A, 14* (1959) 727.
[24] H.L. Tuller and A.S. Nowick, *J. Electrochem. Soc., 126* (1979) 209.
[25] D.J.M. Bevan and J. Kordis, *J. Inorg. Nucl. Chem., 26* (1964) 1509.
[26] W. Noddack and H. Walch, *Z. Phys. Chem., 211* (1959) 194.
[27] C.J. Kevane, E.L. Holverson and R.D. Watson, *J. Appl. Phys., 34* (1963) 34.
[28] R.R. Heikes and W.D. Johnston, *J. Chem. Phys., 26* (1957) 582.
[29] R.M. Berman, *Rep. No. W.A.P.D.-316, Bettis Atomic Power Lab., Pittsburgh,* PA, USA, 1967.
[30] R.J. Ackermann, R.J. Thorn and G.H. Winslow, *J. Opt. Soc. Am., 49* (1959) 1107.
[31] B.T.M. Willis, *Proc. R. Soc. London, Ser. A, 274* (1963) 134.
[32] G.C. Allen and P.A. Tempest, *J. Chem. Soc., Dalton Trans.,* (1982) 2169.
[33] T.R. Griffiths, H.V.St.A. Hubbard, G.C. Allen and P.A. Tempest, *J. Nucl. Mater., 151* (1988) 307.
[34] T.R. Griffiths, H.V.St.A. Hubbard, G.C. Allen and P.A. Tempest, *J. Chem. Soc., Faraday Trans. 1, 84* (1988) 4377.
[35] P.A. Tempest, P.M. Tucker and J.W. Tyler, *J. Nucl. Mater., 151* (1988) 251.
[36] E.F. Westrum and F. Gronvold, *J. Phys. Chem. Solids, 23* (1962) 39.